Andrea Montgomery was born in Fort Dodge, IA and grew up in Omaha, NE. She attend Butler University in Indiana, majoring in physics, and minoring in math and music. After graduation, she participated in a SULI internship at Lawrence Berkeley National Lab. She currently is enrolled in a PhD program at the University of Wisconsin, Madison, studying plasma physics. Her hobbies include singing and cooking.

Carl Schroeder is a staff scientist at the Lawrence Berkeley National Laboratory (LBNL). He received his Ph.D. in physics from the University of California at Berkeley in 1999 for his study of intense, short-pulse, laser-plasma interactions. Following postdoctoral work studying x-ray free-electron lasers at UCLA and SLAC, he joined the Accelerator and Fusion Research Division of LBNL in 2002. At LBNL his research activities have focused on the development of laser-driven plasma-based accelerators and novel radiation sources.

Studies of a Free Electron Laser Driven by a Laser-Plasma Accelerator

Andrea Montgomery, Carl Schroeder, and William Fawley

ABSTRACT

A free electron laser (FEL) uses an undulator, a set of alternating magnets producing a periodic magnetic field, to stimulate emission of coherent radiation from a relativistic electron beam. The Lasers, Optical Accelerator Systems Integrated Studies (LOASIS) group at Lawrence Berkeley National Laboratory (LBNL) will use an innovative laser-plasma wakefield accelerator to produce an electron beam to drive a proposed FEL. In order to optimize the FEL performance, the dependence on electron beam and undulator parameters must be understood. Numerical modeling of the FEL using the simulation code GINGER predicts the experimental results for given input parameters. Among the parameters studied were electron beam energy spread, emittance, and mismatch with the undulator focusing. Vacuum-chamber wakefields were also simulated to study their effect on FEL performance. Energy spread was found to be the most influential factor, with output FEL radiation power sharply decreasing for relative energy spreads greater than 0.33%. Vacuum chamber wakefields and beam mismatch had little effect on the simulated LOASIS FEL at the currents considered. This study concludes that continued improvement of the laser-plasma wakefield accelerator electron beam will allow the LOASIS FEL to operate in an optimal regime, producing high-quality XUV and x-ray pulses.

Introduction

As researchers work to understand properties of materials on the molecular and atomic level, new instruments must be developed that are both accurate and powerful at nanometer and femtosecond scales. One option is the free electron laser (FEL), a device that uses a periodic magnetic field and electromagnetic radiation (either from a seed laser or spontaneous emission) to stimulate the emission of coherent radiation from a relativistic beam of electrons. The Lasers, Optical Accelerator Systems Integrated Studies (LOASIS) group at Lawrence Berkeley National Laboratory (LBNL) is developing such an instrument. An FEL must be driven by an energetic, high-quality, relativistic electron beam in order to lase at the desired wavelengths. Over the past several years, the LOASIS group has developed laser-plasma wakefield accelerator (LWFA) technology, allowing compact generation of these electron beams [1]. The LWFA electron beam is ultra-short (approximately 50 fs) with a mean energy up to 1 GeV, and a small projected energy spread [2]. With the LWFA electron beam, the FEL will be able to produce ultra-short laser pulses at UV and x-ray wavelengths. A laser with these properties will allow researchers to explore ultra-fast phenomena such as chemical reactions and phase-transitions of materials using pump-probe experiments.

As the LWFA is being tested and developed at LBNL, the FEL is being designed. Consequently, members of LOASIS must not only optimize the performance and improve the analysis of the electron beam from the laser-plasma accelerator, but also must address any problems or non-ideal conditions that might seriously affect the FEL performance. The FEL simulation program GINGER is used to model a wide range of FELs, including those with certain non-ideal effects. It can predict how the FEL will perform and identify problem issues prior to running the experiment.

Modeling of the LOASIS FEL is focused on optimizing its performance at wavelengths and powers compatible with the LWFA, and also predicting the effects of phenomena such as wakefields and mismatched beams. Some important electron beam parameters include energy spread, transverse emittance, and the interrelated quantities of current, charge, and pulse length. Knowledge of what type of electron beam creates good FEL performance provides LWFA researchers with realistic benchmarks for success. Wakefields, the electromagnetic fields caused by high-current electron bunches moving through the slightly resistive vacuum chamber, have the potential to reduce the output power of the laser. Consequently, it is useful to study the scaling of wakefields with FEL parameters and determine at what point they will become a severe detriment to the laser performance. Another possible problem is electron beam

mismatch to the undulator focusing lattice. This could occur when the electron beam entering the FEL system has the wrong transverse size or when it is diverging or converging. The magnitude of the effects caused by these imperfections can help determine the types of transport optics to be used between the LWFA beam source and the FEL beam entrance.

Analysis has also included effects on the output at the third harmonic of the resonant wavelength. Although it produces much lower power than the fundamental wavelength, the third harmonic emission provides a way to reach shorter wavelengths while still operating within the range of the current LWFA and FEL experimental configuration (i.e., beam energy and undulator wavelength).

This paper presents an overview of the simulation code GINGER, including the approximations used, and analysis of the results obtained from this code for the LOASIS FEL. These analyses include a range of optimal values for energy spread and emittance, a discussion of the most effective method for reaching short wavelengths, and an overview of the predicted effects of wakefields and mismatched beams.

Materials and Methods

GINGER is a multidimensional simulation code that tracks macroparticles, each of which represents numerous actual electrons. These macroparticles interact with electromagnetic fields which vary both radially and along the undulator axis. GINGER uses the slowly-varying envelope approximation of Maxwell's equations (also known as the eikonal approximation) and undulator-period averaged FEL equations for advancing the electromagnetic fields. The code simultaneously determines the value of the bunched transverse electron current and advances the macroparticles' energies and longitudinal phases as they move along the undulator. For more information on GINGER, see Fawley [6].

GINGER has the capability to run in two different modes. The first is a simple, monochromatic approximation that requires relatively little computational expense, allowing the user to scan over a large number of parameters in a short amount of time. This mode uses only one slice of macroparticles to model the entire duration of the pulse. GINGER tracks this single slice as it moves down the length of the undulator. By recording the fundamental and third harmonic power output at the end of the undulator for series of runs in which individual parameters are varied, the functional dependence of the FEL performance upon these parameters can be determined. Sample parameters include the energy spread, normalized transverse emittance, peak current, and matching parameters of the electron beam and the resonant wavelength of the system. Scanning in time-independent mode helps define a reasonable range of parameter values that result in lasing. A more accurate simulation can then be run in the second, more accurate GINGER mode.

The second mode in GINGER is fully time-dependent (and polychromatic) with respect to the electron pulse and radiation field, tracking multiple slices of macroparticles and fields in order to cover the full duration of the electron pulse. Using predictions and measurements of the LOASIS LWFA electron source, it is estimated that electron pulse durations will be approximately 30 fs long. To model the FEL, GINGER subdivides this pulse longitudinally, with each slice on the order of half a femtosecond long. These slices are then tracked as they move down the undulator. Time-dependent mode allows proper simulation of self-amplified spontaneous emission (SASE). SASE, which is initiated by random microbunching (i.e. shot noise) on the electron beam as it enters the undulator, does not require a seed laser at a specified wavelength, and is tunable by changing the initial electron energy or the magnitude of the undulator magnetic field. The spontaneous emission is created in the simulation using two user-input random number seeds for the microbunching. For most cases, the $RANDOM function in UNIX was used to generate these seeds.

Time-dependent mode is also needed to study the effects of vacuum chamber wakefields as they vary in time. To create realistic wakefields, a separate code generates the electric field in the longitudinal direction as a function of time relative to the passing electron bunch. GINGER then uses this additional electric field as it advances Maxwell's equations for the macroparticles' energies along the undulator axis.

Results

Studies of the proposed FEL center around one nominal case, the parameters of which are shown in Table 1 [3]. The GINGER runs presented use these parameters unless specified otherwise. For further information on the undulator construction and configuration, see Robinson et al [5]. The first parameter to be studied was energy spread. This value is defined as the ratio of the RMS variation in energy to the peak energy of the electron beam. Ideally, the energy spread will be as small as possible. The measured projected energy spread of the LOASIS LWFA electron beam is on the order of one percent [1]. The instantaneous energy spread may be much smaller than the projected spread, which is integrated over time. In addition, refinements in the LWFA design should allow

LWFA electron beam:	
Beam energy, γmc^2	0.5 GeV
Peak current, I (seeded/SASE)	5 kA / 10 kA
Longitudinal bunch shape	parabolic
Bunch duration (Full width)	30 fs
Charge	0.15 nC
Energy spread (slice, RMS), σ_γ/γ	0.25%
Normalized transverse emittance	1 mm mrad
Undulator:	
Undulator wavelength, λ_u	2.18 cm
Minimum magnetic gap	4.8 mm
Resonant wavelength, λ_s	31 nm
Seed Laser (when applicable):	
Radiation wavelength	31 nm
Radiation power	15 MW

Table 1. Nominal Parameters for GINGER Simulations.

production of electron beams with less than 0.5% energy spread. The range examined for FEL simulations went from 0.01% to 0.7%, with 0.25% being the value used for GINGER scans of other parameters (see Table 1). The output power for the fundamental wavelength and the third harmonic as a function of initial energy spread are shown in Figure 1(a,b). The second electron parameter scanned was normalized transverse emittance. Transverse emittance is a measure of the beam's area in transverse phase space (as shown in Figure 2) and is related to the product of the beam's radius and its transverse kinetic temperature. A large transverse emittance can affect the beam size as it is focused and also leads to an increase in the spread of beam particles' longitudinal velocity. Normalized transverse emittance is defined as $e_n = \gamma\sqrt{\langle\theta^2\rangle}\sqrt{\langle r^2\rangle}$. The nominal value for the LOASIS beam is 1 mm mrad, and the range of values scanned was from 0.2 mm mrad to 4.0 mm mrad. The output powers are shown in Figure 3(a,b).

Studies of the effects of a mismatched electron beam were also performed in the quick, time-independent mode of GINGER. The first parameter, α-Twiss, ranges from -1 to 1, and is a measure of the divergence of the beam, with -1 indicating a diverging beam, and +1 indicating a converging beam. The resulting output radiation power for the fundamental is shown in Figure 4. The second mismatch parameter is the scaled β-Twiss, which is a factor related to the cross-sectional size of the beam. Specifically, for these simulations, RMS beam size = $60\mu m \cdot \sqrt{\beta_{Twiss}}$. When β-Twiss = 1, the beam is ideally matched to the undulator focusing, with an RMS beam size of 60 μm, which stays constant for the length of the undulator. When β-Twiss < 1, the beam is too small, and when β-Twiss > 1, the beam is too large. Here, β-Twiss is varied from 0.25 to 4.0 (with RMS beam size ranging from 30–120 μm), as shown in Figure 5.

In order to study the possibilities for using the third harmonic to reach shorter wavelengths than are possible with the fundamental only, two series of runs were performed. In the first, the fundamental resonant wavelength varied from 12 nm to 31 nm. In order to change the resonant wavelength, λs, the strength of the normalized peak magnetic field of the undulator, a_w, was increased, in accordance with the FEL resonance relationship: $\lambda_s = \lambda_u (1 + a_w^2) / (2\gamma^2)$, where γ is the energy of the beam in units of mc^2 and λ_u is the undulator wavelength. The radiation power output for both the fundamental as it ranges from 12 nm to 31 nm and the associated third harmonic, ranging from 4 nm to 10.3 nm are plotted in Figure 6. In order to reach third harmonic wavelengths exceeding 10.3 nm, a different variable in the FEL resonant relationship may be varied. The maximum undulator magnetic field is limited by the allowed magnetic gap in the configuration, so for fundamental wavelengths larger than 31 nm, the energy of the beam must be decreased to increase the wavelength. Similar runs were performed using SASE as the initial radiation source instead of a seed laser (see Figure 7). In order to simulate SASE, the time-dependent mode of GINGER was used. In these cases, changing the magnitude of the undulator magnetic field was the only method explored to vary the resonant fundamental wavelength.

The final studies concerned the effects of wakefields in the vacuum chamber of the undulator. Using a vacuum chamber radius

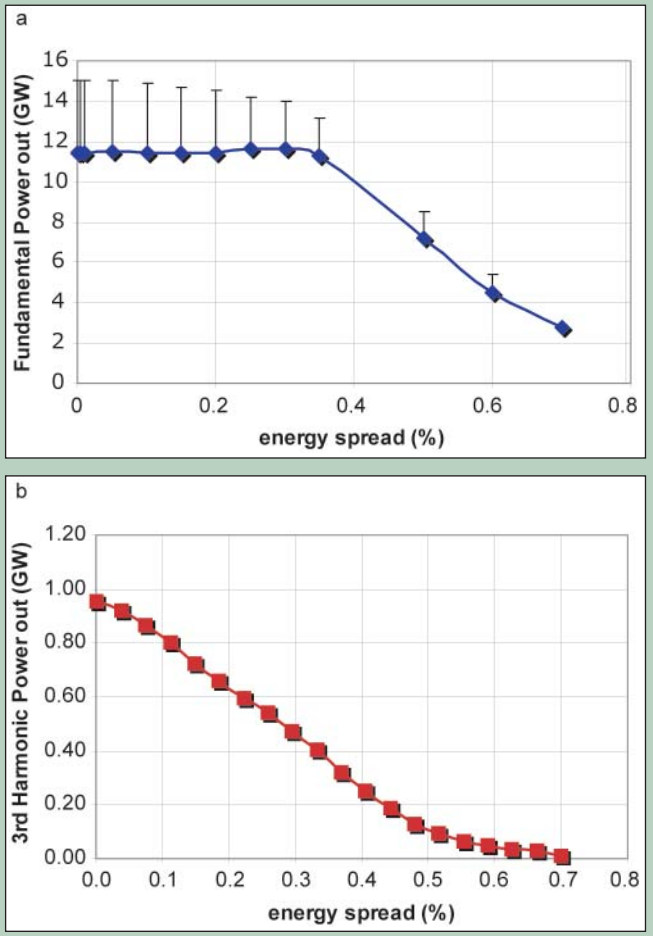

Figure 1. Predicted power vs. initial energy spread at undulator exit (z = 5 m) at a) the fundamental (31 nm), b) the third harmonic for the seeded case. The bars in (a) show the maximum power achieved at saturation.

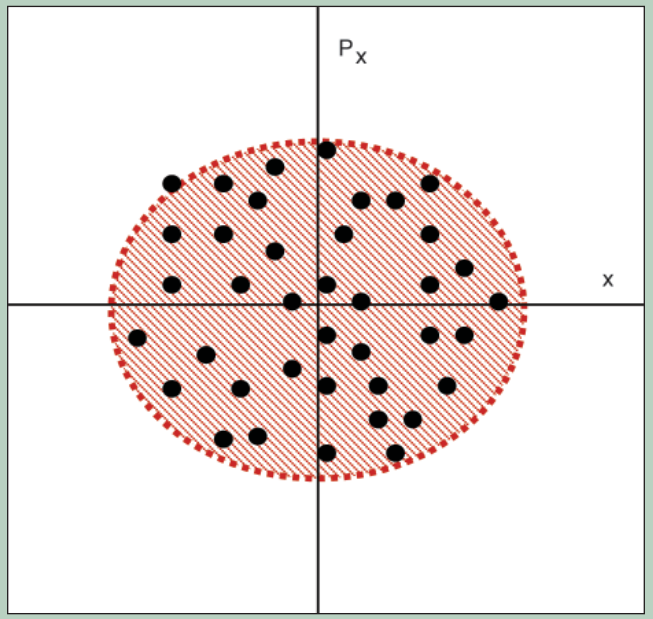

Figure 2. Transverse emittance is related to the RMS (root-mean-squared) aread in transverse phase space. This is the area that encloses a plot of the particles' transverse displacement vs. transverse moment.

of 2 mm, several cases were considered. A basic approximation, for which the conductivity parameters are well known, is to treat the chamber as an aluminum cylinder with AC conductivity. The resulting wakefield from 300 pC of beam charge contained within a bunch length of 30 fs is shown in Figure 8. The actual vacuum chamber for the undulator to be used by LOASIS is constructed from stainless steel 303, for which the DC conductivity is well documented, but for which the AC conductivity relaxation time, τ, is unknown. To deal with this, it was presumed that 303 stainless steel has the same τ as iron, which is well known [4]. Figure 8 also shows the computed wakefields for a stainless steel vacuum chamber with both AC and DC conductivity models. To obtain basic statistical data on the expected effects of wakefields, a series of 32 SASE runs with different random number seeds were compared with 64 statistical SASE runs with no wakefields included. In these runs, the aluminum AC conductivity model was used to compute the wakefield. The resulting RMS values and relative differences are shown in Table 2.

In order to model the effects of current on wakefields, and how that, in turn, affects the electron beam, a series of different wakefields were created for varying currents, I. The pulse length, τ_p, was kept constant, and the charge, Q, was varied to satisfy the equation $I\,\tau_p = Q$. The resulting output energies are compared with the equivalent runs without wakefields in Figure 9.

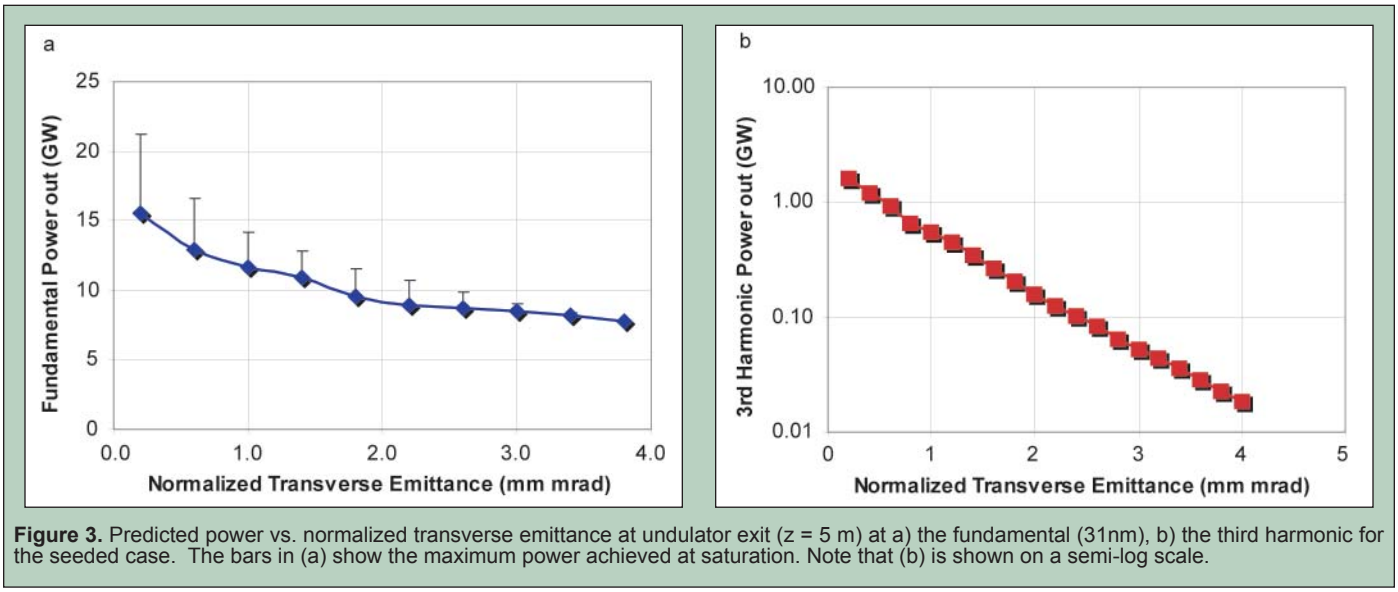

Figure 3. Predicted power vs. normalized transverse emittance at undulator exit (z = 5 m) at a) the fundamental (31nm), b) the third harmonic for the seeded case. The bars in (a) show the maximum power achieved at saturation. Note that (b) is shown on a semi-log scale.

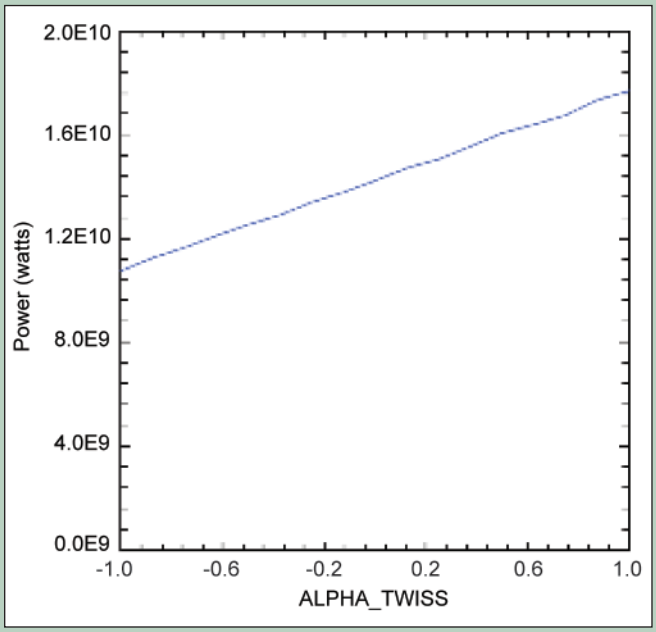

Figure 4. Maximum radiation power vs. α-Twiss, where α-Twiss = α-Twiss (x) = α-Twiss (y).

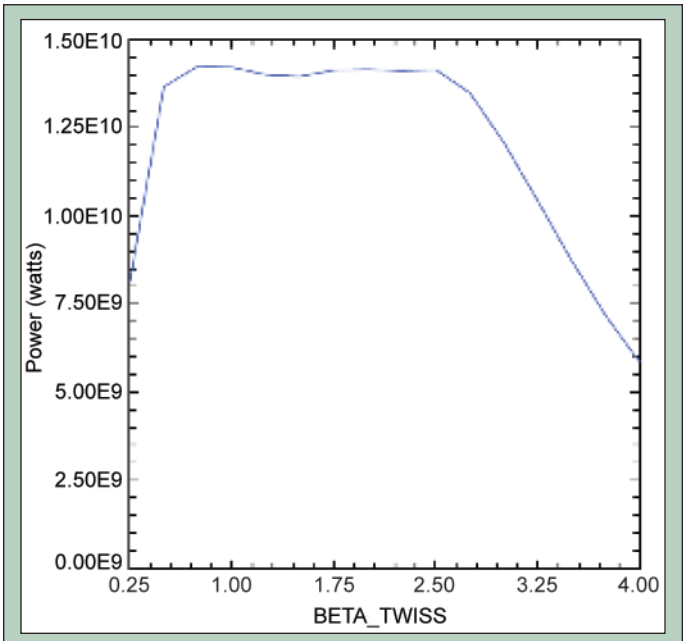

Figure 5. Maximum radiation power vs. the scaled β-Twiss where RMS beam size = $60\mu m \cdot \sqrt{\beta_{Twiss}}$. The RMS beam size shown in the graph ranges from 30 μm to 120 μm.

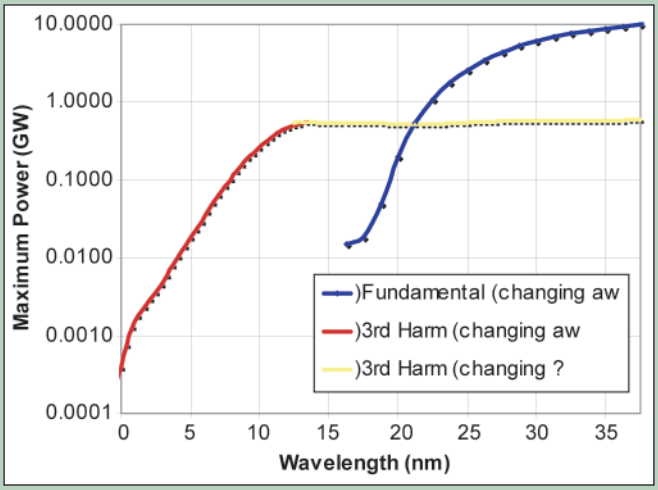

Figure 6. Maximum power at a given wavelength reached using fundamental (blue) and or the third harmonic (red and yellow).

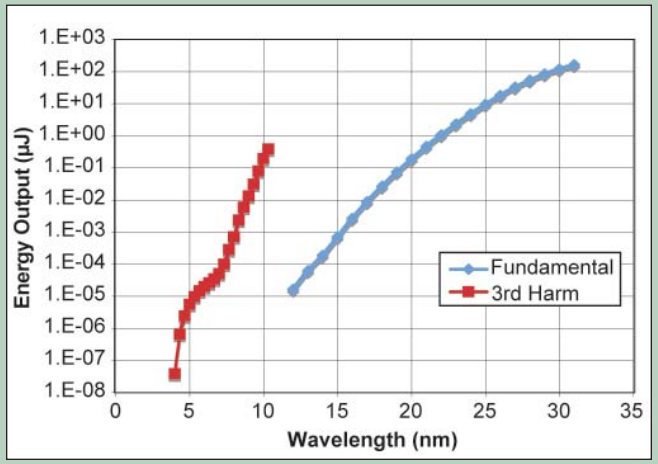

Figure 7. Average energy output vs. resonant wavelength from 4 SASE runs.

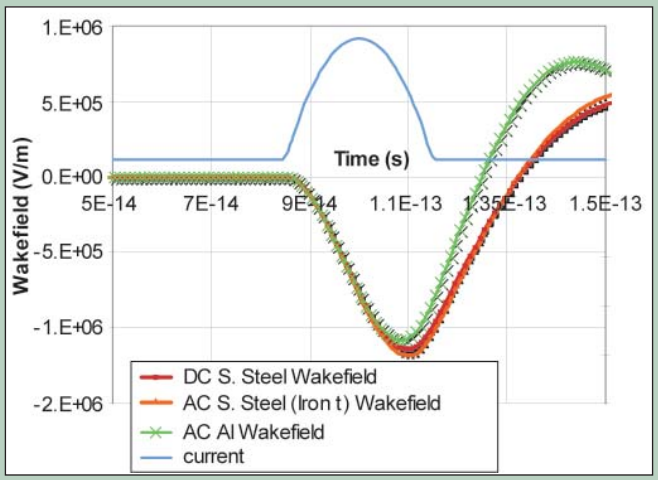

Figure 8. Computed wakefields for DC and AC models for stainless steel (using stainless steel 303 DC conductivity and τ for iron) and aluminum. The current profile is also shown, with peak value of 10 kA. The head of the electron bunch is on the left and the tail is on the right.

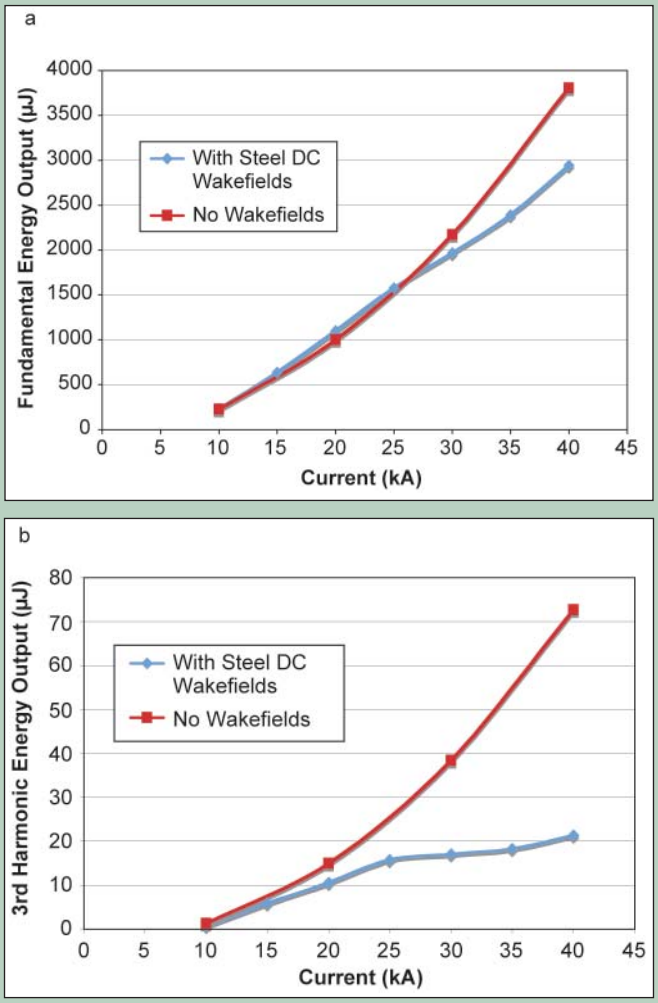

Figure 9. Output energies for a) the fundamental, and b) the third harmonic as current is varied (and pulse length kept constant). This is shown for the case with stainless steel DC wakefields and the case where no wakefield effects were included.

	Fundamental (31 nm)	3rd Harmonic (10.3 nm)
Avg. Output Energy (with wakefields) (μJ)	211.6	0.819
Std. Deviation (with wakefields) (μJ)	61.3	0.443
Avg. Output Energy (no wakefields) (μJ)	238.0	1.173
Std. Deviation (no wakefields) (μJ)	58.8	0.532
Percent Difference between output energies $(E_{no\ wake} - E_{wake}) / ½ (E_{no\ wake} + E_{wake})$ (100%)	11.8	35.6

Table 2. Statistical Analysis of Wakefield Effects for Nominal Case.

Discussion and Conclusions

These studies help provide a better understanding of the parameters needed to obtain successful FEL with the LOASIS electron beam and some of the expected properties of the resulting laser. The relative energy spread per slice has a clear effect on the fundamental power, as seen in Figure 1a. For an energy spread less than 0.35%, the laser can saturate (reaching its maximum power) before the end of the undulator, and then slowly oscillates near that power until the undulator exit. For an energy spread of greater than 0.35%, the laser does not saturate by the time it reaches the end of the undulator, and the output power drops linearly as energy spread increases. The third harmonic (as shown in Figure 1b), however, does not have a maximum energy spread below which the power stays approximately constant. Instead, the approximately linear dependence of output power on energy spread continues even for very small energy spreads. The difference in performance between a beam with 0.5% energy spread and 0.25% energy spread was noted for several other cases where other parameters, such as resonant wavelength, were varied.

Examining the scans in emittance in Figure 3, there is no clear cut-off point as there is for energy spread, nor is there a linear dependence of fundamental power on emittance. The nominal value for emittance, 1 mm mrad, gives an acceptable output fundamental power of approximately 12 GW in this seeded run. The third harmonic output power does have an interesting exponential correspondence of output power with emittance that is not yet fully understood.

The maximum power shown in the α-Twiss scan in Figure 4 shows that the FEL performance is relatively insensitive to beam divergence for the parameters considered. Varying β-Twiss gives a definite but large range of beam sizes that will allow the FEL to saturate in the undulator. The results shown in Figure 5 indicate that the RMS beam size could range from 40–100 μm without an appreciable loss of power. Beam mismatch appears to have less of an effect on FEL performance than beam emittance and energy spread.

Even with a matched beam with ideal emittance and energy spread, it is difficult to operate at wavelengths shorter than 31 nm without decreasing the output power. Figure 6 shows that the most effective way to reach wavelengths below 13 nm is to use the third harmonic. Although the maximum power for these is still under a gigawatt, the number of photons reaches a maximum of 7×10^{11}. In the equivalent SASE runs, as shown in Figure 7, we see that wavelengths between 7 nm and 10 nm are best obtained by using the third harmonic. Below 7 nm, the output energy appears to be dominated by spontaneous emission, indicating that no significant bunching (i.e., coherent emission) has occurred.

Wakefields are the final issue addressed in this paper. As can be seen in Figure 8, the three types of wakefields examined (AC aluminum, AC stainless steel, and DC stainless steel) have nearly identical values over the time span occupied by the current. Because of this, all three types of wakefield models yield similar results. All wakefield simulations were run as SASE cases, so numerous runs were done with different random seeds. In Table 2, one sees that a) the third harmonic was affected more by wakefields than the fundamental, and b) that, although there is a statistically important percent difference between the RMS value for the cases with wakefields and those without, both RMS values lie within a standard deviation of each other. Some individual cases with wakefields had better performance than some cases without wakefields, but, on average, output energy was greater for the case without wakefields, as expected. The uncertainty introduced by the randomness of the SASE runs is large enough that it makes the energy loss caused by wakefields experimentally insignificant.

Improvements in the LWFA performance may allow for larger currents, which would in turn create larger wakefields. Figure 9 shows at what current wakefields will begin to have a significant effect on the energy output for the fundamental and third harmonic. In Figure 9a, one can see that wakefields cause a decrease in output energy only at high currents (i.e., above 35 kA). Wakefields have a more significant effect on the third harmonic as seen in Figure 9b, where they significantly decrease the output energy at currents as low as 25 kA.

The results and analysis presented in this paper provide a range of parameters for which the FEL will perform best. The most significant of these parameters is energy spread, which must be small to ensure FEL saturation. It has also been shown that beam mismatch and vacuum chamber wakefields will not have a large effect when the standard input parameters are used. Continued improvement of the LWFA electron beam will allow the LOASIS FEL to operate in an optimal regime and produce a high-quality x-ray laser pulse.

Acknowledgements

This research was conducted at Lawrence Berkeley National Laboratory. Many thanks go to my advisors, Carl Schroeder and William Fawley for their guidance and support. I also thank Florian Gruener for challenging me to understand FEL's and GINGER better. In addition, I thank the members of the LOASIS research group. This work was supported by the Director, Office of Science, Office of Basic Energy Sciences, of the U.S. Department of Energy under Contract No. DE-AC02-05CH11231.

References

[1] C.G.R. Geddes, Cs. Toth, J. van Tilborg, *et al*, "High-quality electron beams from a laser wakefield accelerator using plasma-channel guiding," *Nature*, Vol. 431, 538–541 (Sep 2004).

[2] W.P. Leemans, B. Nagler, A.J. Gonsalves, *et al*, "GeV electron bemas from a centimeter-scale accelerator," *Nature Phys.*, Vol. 2, 696–699 (Oct 2006).

[3] C.B. Schroeder, W.M. Fawley, E. Esarey, and W.P. Leemans, "Design of an XUV FEL Driven by the Laser-Plasma Accelerator at the LBNL LOASIS Facility," in *Proceedings of FEL 2006*, 455–458, JACoW (Sep 2006).

[4] D. Scott, “Longitudinal Resistive Wall Wakefields for the ILC Positron Undulator Vessel,” ASTEC-ID-040 (May 2006).

[5] K.E. Robinson, D.C. Quimby, and J.M. Slater, “The Tapered Hybrid Undulator (THUNDER) of the Visible Free-Electron Laser Oscillator Experiment,” *IEEE Journal of Quantum Electronics*, Vol. QE-23, 1497–1513 (Sep 1987).

[6] W.M. Fawley, Technical Report LBNL-49625, Lawrence Berkeley National Laboratory, (2002).